SPE-212707-MS

SCAL-On-Chip: Measurement and Interpretation of Multiphase Fluid Flow Characteristics in Porous Media. A Microfluidic Approach

Bettina Jenei, Clausthal University of Technology; Roman Manasipov, Datagration Solutions Inc; Nils Langanke and Hanin Samara, Clausthal University of Technology

 DOI 10.2118/212707-MS

This paper was prepared for presentation at the SPE Reservoir Characterisation and Simulation Conference and Exhibition held in Abu Dhabi, UAE, 24 - 26 January 2023.

Abstract

This work aims to conduct, interpret and derive the multi-phase fluid flow behaviour more efficiently and feasibly from a novel perspective. The goal is to conduct a SCAL measurement using a microfluidic setup on a chip and interpret the in-situ results, where the parameters influencing the multi-phase fluid flow in porous media, such as wettability, capillary pressure, and relative permeability, are measured simultaneously. There are numerous economic and technical advantages of this approach. Conventionally, SCAL measurements are conducted through core samples using X-ray and multi-phase fluid flow parameters in porous media are measured separately. These properties can be simultaneously determined in digital rock physics (DRP) by applying micro-CT imaging but with high costs. The steady-state method was utilised in this study and re-designed for microfluidic flooding. The measurement was conducted using one oleic and one aqueous phase, applying different fractional flow steps, mimicking the range of varying water saturation in the reservoir during the depletion process. The used microchip has a synthetic pore-structure design with circular grain shapes. The measurements conducted are visible in real-time using a microfluidic approach. The experimental results show that it is possible to adapt the microfluidic flooding for conducting and interpreting SCAL measurements. An additional advantage of this method is that the wettability and capillary pressure could be successfully determined by means of image processing using only the data obtained from the steady-state method in a microchip. Since the measurements are visible live, and images of the microchip are captured with the desired frequency, the image processing facilitates the understanding and interpretation of multi-phase fluid flow in porous structures, which is not possible with cores. Overall, to overcome the technical and economic limitations of digital rock physics, the application of SCAL through microchips representing the porous media is a good alternative. The SCAL-on-Chip is a promising approach for describing and analysing multi-phase fluid flow. Image processing contributes to developing "smarter" and cheaper interpretation tools for estimating wettability and capillary pressure. It provides the possibility to derive mathematical models of the relationship between multi-phase flow characteristics. The derivation of a general function between the measured properties could be possible with machine learning and a sufficient amount of experiments using pore structures that closely resemble porous media.

Introduction

In the past few decades, the demand for energy has grown drastically. While the supply lasts, new methods and technologies need to be investigated to prolong the lifespan of available reserves. Several recovery methods have been proposed to enhance the recoverability of trapped hydrocarbons in the reservoir. These methods encompass gas, thermal and chemical enhanced oil recovery technologies. The success of these methods necessitates the understanding of multi-phase flow in porous media and the governing mechanisms involved in changing fluid saturation and fluid distribution in the reservoir. There are two key parameters describing the fluid flow characteristics in permeable media, namely the relative permeability $k_r(Sw)$ and capillary pressure $P_c(S_w)$. Their measurements are traditionally performed through special core analysis (SCAL), which is time-consuming and costly, and the outcome is not always of the best quality (Blunt, 2017). Traditional SCAL conducted through core samples using the differential core-flooding setup, centrifuge and X-ray is where the two functions of interest are measured separately (McPhee et al., 2015). However, these properties can be more thoroughly and simultaneously determined in digital rock physics (DRP) by applying micro-CT imaging which is associated with high costs based on (Blunt et al., 2013) and (Gao et al., 2017).

In order to perform a more economically feasible multi-phase fluid flow experiment, the microfluidic method has been proposed. The microfluidic approach through microchips has already proven to be an appropriate solution in analysing and verifying the success of numerous enhanced oil recovery (EOR) techniques (Wegner, 2015), such as polymer flooding, surfactant flooding and microbial EOR, to name a few (Tahir et al., 2020), (Mejia et al., 2019), (Khajepour et al., 2014). The success of this method lies in the real-time visualisation of the fluid displacement process as well as fluid saturation profiles without the need to resort to X-ray or microCT imaging. In this method, images of the microchip are sequentially recorded during the experiment at the desired frequency. With the help of image processing software, the understanding of the multi-phase fluid flow in porous structures at a pore scale and the consequent interpretation of the findings is facilitated, thereby unravelling the mystery associated with the traditional measurements through cores.

In this paper, a special core analysis (SCAL) method is employed using a microfluidic setup on a chip, and the in-situ results are interpreted. The measurement and interpretation of relative permeability and capillary pressure curves as a function of saturation using SCAL on Chip constitutes the first objective of this work. The second objective is to verify the suitability of the method as an alternative to conventional time-consuming, and costly methods. This method should serve as an additional means of performing relatively fast measurements, utilising minimum volumes of reservoir fluids and minimising energy consumption per experiment.

Materials and Methods

In order to measure and analyse the different parameters from only one steady-state measurement, two additional traditional measurements were required. The relative permeability interpretation requires viscosity measurements, which were done by using a rheometer. The relative permeability values are interpreted analytically with the utilisation of extended Darcy's law for both phases.

$$q\alpha = -\frac{k_{r\alpha}k_{\alpha}}{\mu_{\alpha}} A \nabla p_{\alpha} \quad \text{Eq. 1}$$

, whereq_{α} – flux of phase α, $k_{r\alpha}$ – relative permeability of phase α, k_{α} – absolute permeability, μ_{α} – viscosity of phase α, A – cross-sectional area of the fluid flow, ∇p_{α} – pressure gradient of the fluid phase α, and phase α can be oil or water.

There is a difference between the individual fluid phase pressures and that is because of the existence of capillary pressure, which, therefore can be written as follows:

$$P_{cnw-w} = p_{nw} - p_w \quad \text{Eq. 2}$$

, where $P_{(cnw\text{-}w)}$ – capillary pressure between non-wetting and wetting phase, p_{nw} – non-wetting phase pressure, p_w – wetting phase pressure.

One of the goals is to measure the contact angle (Andrew et al., 2014a) in order to calculate the imbibition capillary pressure function. In a multi-phase fluid system within a porous media, the contact angle can be described by the interfacial tensions between the participating phases (brine-oil-rock), by Young's equation (Eq. 3).

$$\cos\theta = \frac{\sigma_{so} - \sigma_{sw}}{\sigma_{ow}} \quad \text{Eq. 3}$$

, where θ – contact angle, σ_{so} – solid-oil tension, σ_{sw} – solid-water tension and σ_{ow} – oil-water interfacial tension.

Additionally, for the calculation of capillary pressure at each fractional flow step with the determination of the contact angles through image analysis, the interfacial tension between the two used fluids must be measured. In this work, the standing drop method was used to measure the interfacial tension of the water-oil system.

Materials

The utilised fluids are an oleic and an aqueous phase. The oleic phase originates from southern Mexico, and as the aqueous phase, distilled water was used. The reason for running the measurements with distilled water was to eliminate the impact of brine salinity on wettability, which could be encountered with the reservoir brine.

Microfluidic experimental apparatus

The traditional steady-state experiment is selected and adjusted for microfluidic flooding in this work. It is possible to adapt the experimental setup of microfluidics with a chip for conducting and interpreting SCAL measurements (Ghazanfari et al., 2006). The measurements were conducted using one oleic and one aqueous phase (deionised water) under atmospheric pressure and 40 ˚C. An oven maintains a constant temperature. Digital Single-Lens Reflex (DSLR) camera makes the measurements visible in real time. The experiments were conducted on a single microchip. The schematic diagram of the SCAL-on-chip experimental setup is shown in Figure 1.

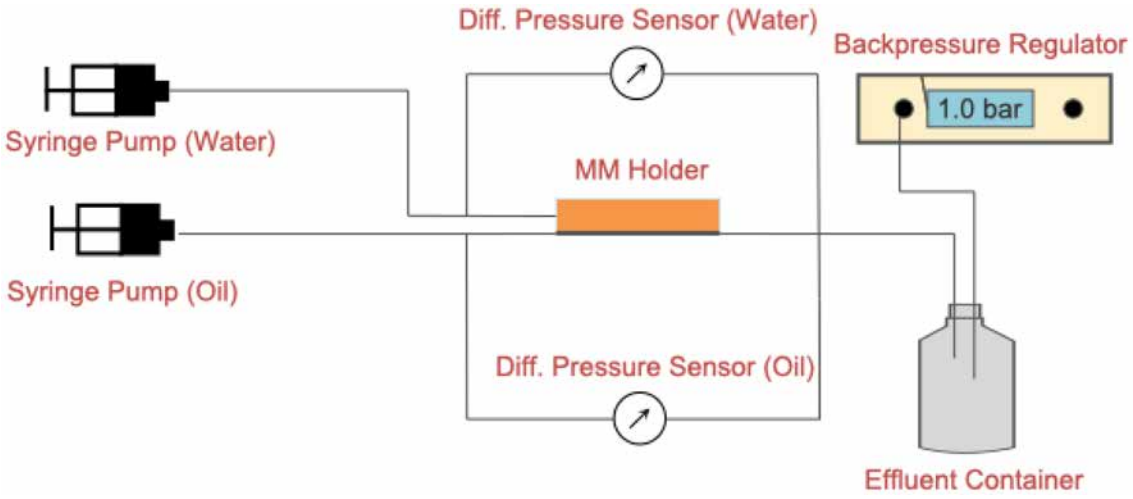

Figure 1—Schematic diagram of MMSCAL (Micromodel SCAL) setup

Further details about the microfluidic approach can be found elsewhere (Wegner, 2015). The chip resembling porous media had a synthetic design with spherical grain shapes with relatively high permeability. The selected chip design is based on a circular grain shape with linear random distribution, making this chip an appropriate candidate for contact angle measurements due to its synthetic silica surface.

The chip is 4 cm in length, the cross-sectional side is 0.9 cm, the thickness is 50µm, and the total pore volume is 5µl. Figure 2 shows the grain shape design of the micromodel, and Table 1 summarises the parameters of the applied microchip.

Table 1—MMSCAL synthetic pore-structure design with circular grain shapes of various sizes

MMSCAL Linear Circular			
	[µm]	[mm]	[m]
Length	40000	40	0.04
Width	9000	9	0.009
Thickness	50	0.05	0.00005
	[-]	[%]	
Porosity	0.276	27.6	
	[µl]	[mm³]	[m³]
Pore Volume	4.968	4.968	4.97E-09
	[D]	[mm²]	
Permeability	5	4.93462E-12	

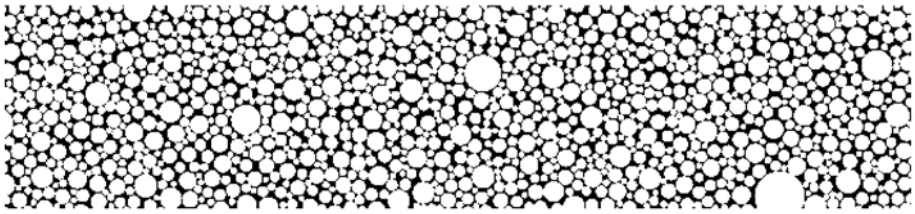

Figure 2—MMSCAL synthetic pore-structure design with circular grain shapes of various sizes

The used chip is designed and proven to be water wet; since it is a synthetic glass-silica-glass chip, there is no varying chemical composition like in real rock. Therefore, it simplifies the confounding effects of mineralogical heterogeneity, a principal cause of contact angle variation. Therefore, the contact angle change could be purely related to the changing fluid deposition velocities during the experiment (Samara & Jaeger, 2022).

Steady State Method

The measurement of relative permeability and capillary pressure values were measured methodologically based on the theory of a typical steady-state SCAL routine, based on the described workflow in (Mcphee, 2015) and (Masalmeh et al., 2015). The work conducted was not limited to the number of data points measured in the publication of Masalmeh (Masalmeh et al., 2015), and the fractional flow steps were adjusted to the scale of the examined problem accordingly. The different water saturations, which mimic the range of variations during the depletion process in the reservoir, were achieved with different fractional flow steps.

The main challenge was to overcome the instabilities produced by the small volumes injected. The total flow rate was constant at 3 µl/min, and the fractional flow (f_w) values varied sequentially from 2%, 4%, 6%, 8%, 10%, 15%, 30%, 50%, 70%, 80% 85%, 90%, which are followed by the 100% water rate and then three bump floods, in order to eliminate the possible capillary end effect. The reason behind the small f_w values is that rapid water saturation increase was experienced only with the 10% water injection level; approximately half of the oil was displaced. It means that the part that interests reservoir engineering calculations during most of the oil field's life is what happens to the multi-phase fluid flow during that period. The more thorough analysis shows success since there are more data points gained from this experiment, and these data points should be revealed in comparison to the previous interpolation between the two data points with fewer measurement points. One of the main reasons to use the steady-state method instead of the faster and simpler unsteady-state method is the density of the gained data points from this specific technique.

The key to performing the steady-state relative permeability measurements in cores and micromodels is to choose the fractional flow values accordingly. This means that with an amount of f_w increase, a proportional amount of water saturation should be changed (increased).

Methods of Image Analysis

One of the main reasons for applying the microfluidic methods in SCAL is the ease with which observing the process visually can be achieved. This feature allows measuring additional properties in comparison to conventional SCAL analysis. Therefore, for various measurements, image analysis is required. This includes the estimation of porosity, aqueous and oleic phase saturations, and contact angles. Automated image processing was done using several Python libraries such as OpenCV (Bradski, 2000), Pillow (Clark, 2015) and scikit-image (der Walt et al., 2014).

Porosity and fluid saturations

To estimate the porosity of the micro-model and to measure fluid saturations at each equilibrium stage, the segregation of colours approach was applied. For that purpose, the image was converted to HSV colour space (Hue Saturation Value) and corresponding colour masks were used to extract the colours of interest. The aqueous phase is captured by the tones of white and blue, the oleic phase by the tones of red, and the solid is represented by the black colour. After applying each mask to the image, the corresponding amount of pixels representing each phase was used to calculate saturations and, similarly, the porosity.

$$S_w = \frac{n_w}{n_w + n_o},\ S_o = 1 - S_w,\ \phi = \frac{n_w + n_o}{n_t} \qquad \text{Eq. 4}$$

, where n_w is the number of pixels representing the aqueous phase, n_o – oleic phase, and n_t – the total amount of pixels representing the micromodel.

For better accuracy, the image beforehand was pre-processed by applying uniform brightness adjustment using flat field correction and histogram equalisation approach (CLAHE – Contrast Limited Adaptive Histogram Equalisation). The automated measurement of saturations allows the recovery of the saturation profiles along the chip length, as well as the calculation of saturations in a two-dimensional lattice.

Contact angle and capillary pressure

Another application of image analysis was related to the measurement of contact angles. At the equilibrium stage of each applied fractional flow, several characteristic contact angles were measured using the edge detection method and polygon fitting approach. The fitted polygon was differentiated to obtain the desired contact angle at specific locations. To calculate the corresponding capillary pressure, the averaged value of contact angles and representative radii of curvature was used. Using the radius of curvature in the horizontal and vertical plane of the micromodel, the equation for capillary pressure calculation at each fractional flow step can be written as follows:

$$p_c = \left(\frac{1}{R_1} + \frac{1}{R_2}\right) \cdot \sigma \cdot \cos\theta_{\text{avg}} \quad \text{Eq. 5}$$

, where R_1,R_2 are the radii of curvature in the horizontal and vertical plane of micromodel, θ_{avg} – average contact angle, σ – interfacial tension.

Measurements of fluid viscosities and IFT

Measurement of the relative permeability requires knowledge of the viscosity of the oleic phase. The viscosity measurements were conducted using a rotational Kinexus rheometer at varying temperatures and 1 atm. The measured viscosity value at 40 ˚C was taken since that was the applied temperature condition during the relative permeability measurement. The results of the conducted viscosity measurements at different temperatures are summarised in Figure 3.

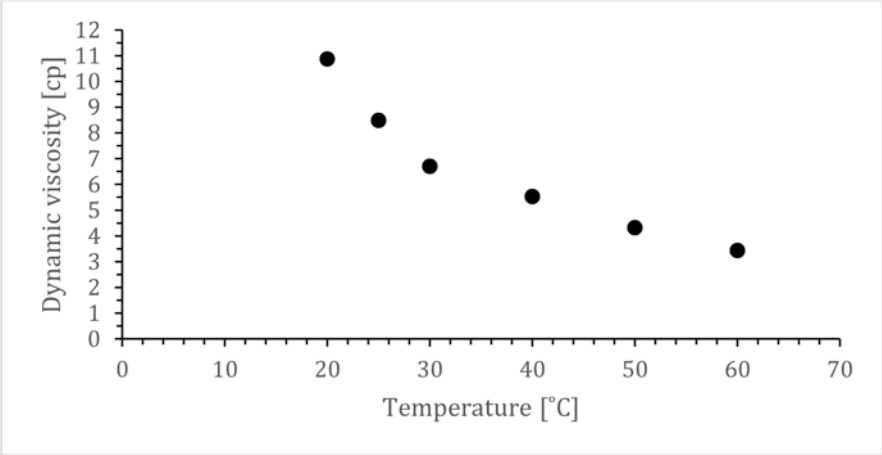

Figure 3—Viscosity of the light oil sample

Interfacial Tension

For the calculation of capillary pressure, the interfacial tension between the two used fluids must be measured. A drop-shape analysis apparatus was used to investigate the interfacial tension (IFT) of a binary crude oil-water system. The IFT was measured using the standing drop method at standard conditions. The schematic diagram of the drop shape analysis setup is shown in Figure 4. Further details about the method can be found elsewhere (Samara et al., 2022). A glass cuvette was filled with double-distilled water, and a drop of oil was formed at the tip of a J-shaped capillary needle that extends into the cuvette. A high-resolution camera connected to a computer records images of the drop as a function of the drop age. The computer is aided with the Axisymmetric drop shape analysis (ADSA) program, which evaluates the IFT based on the Young-Laplace pressure difference across a curved fluid interface. Since knowledge of the densities of the participating phases is important for IFT evaluation, the density of the oil was experimentally measured, and the density of the water was obtained from the National Institute of Standards and Technology (NIST) database. The measurement was performed in triplicates and the average equilibrium value is reported in this work. The maximum relative standard deviation is calculated to be ±2%. The standing bubble is shown in Figure 5.

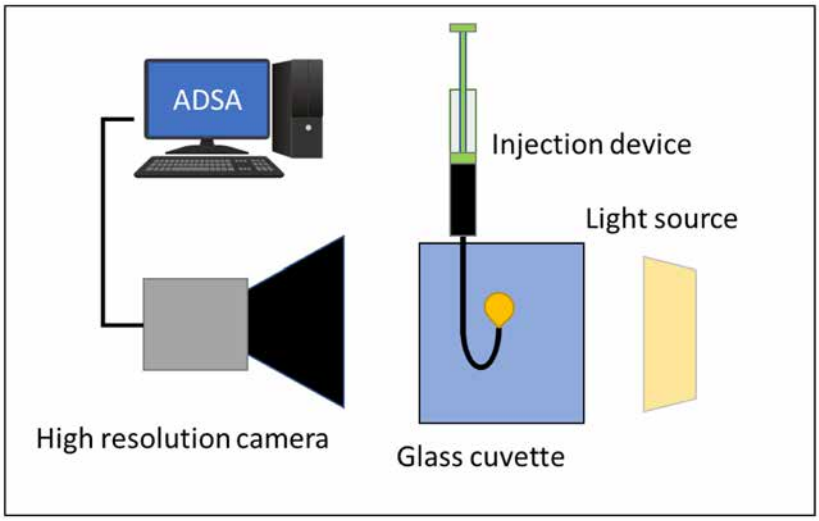

Figure 4—Schematic diagram of the drop shape analysis apparatus.

Figure 5—Standing bubble of crude oil in double distilled water at standard conditions.

The IFT of the binary crude oil-water system is measured to be 14.6 mN/m at equilibrium. The IFT shows dependence on the drop age signifying the presence of surface-active components in the crude, which diffuse towards the interface, ultimately causing the observed drop in IFT. A similar observation is reported in (Oldenburg et al., 2019) and (Yang et al., 2005). The time dependence of IFT is exemplarily depicted in Figure 6.

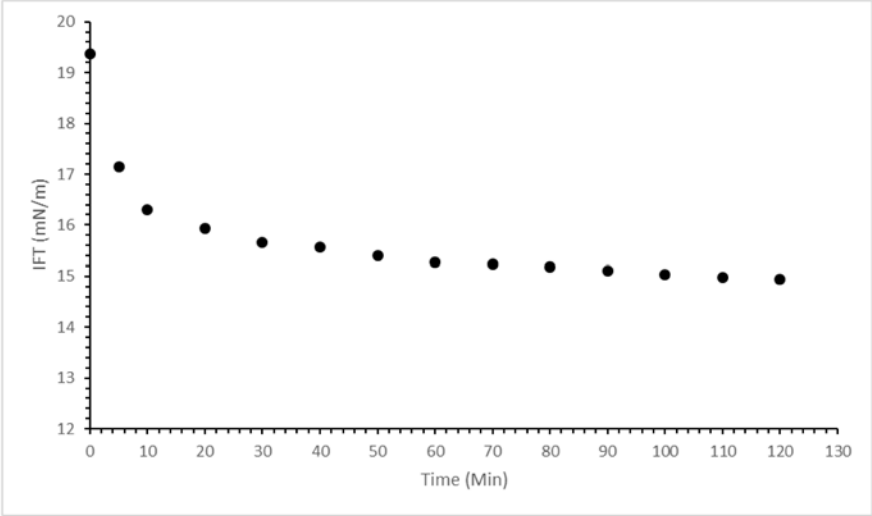

Figure 6—Time dependence of the crude oil-water IFT

Results and Discussion

The steady-state method aims at reaching the equilibrium condition at each fractional flow stage. The differential pressure values for both the oleic and aqueous phases were measured and recorded for the entire duration of the experiment. The images were captured at each steady-state stage. Additionally, the images were saved at ten minutes frequency in order to further analyse the physical phenomena in the observed pressure fluctuations. The initial fluid distribution is illustrated in Figure 8.

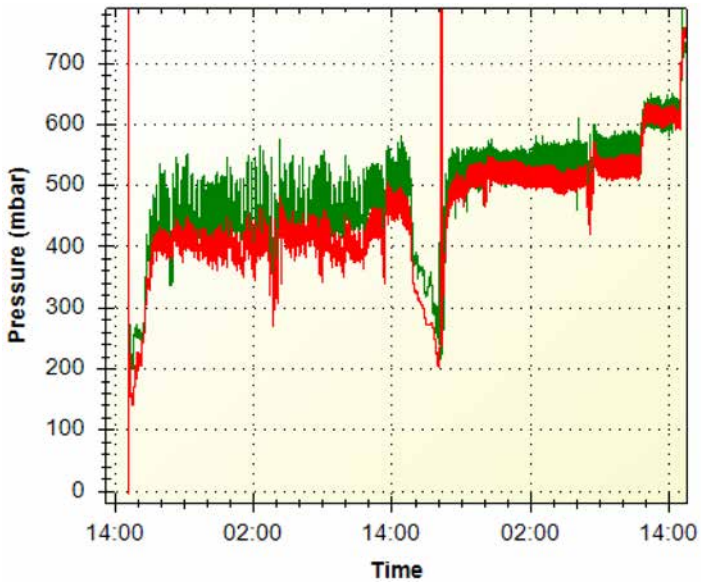

Figure 7—Example of typical pressure recordings at fractional flow (f_w) steps of 10%, 15%, 20% and 30%

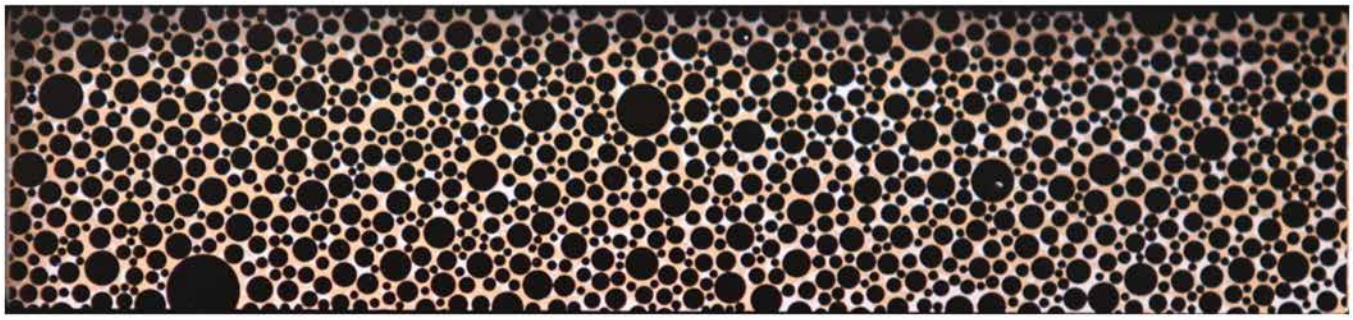

Figure 8—Example of initial oil and water saturation distribution in equilibrium

Differential pressure measurements

Fundamentally, the pressure difference within one fluid phase must be taken when the fluid flow is continuous. At different fractional flow steps, fluctuations occur in the pressure measurements with different amplitudes.

These phenomena can occur on a pore scale due to the ganglion dynamics, which results in the presence of water banks followed by oil banks, which occurs after a sequence of snap-off effects. The application of averaging techniques helps the transition to Darcy's law. Nevertheless, one needs to be careful when interpreting the pressure result at the different fractional flow steps and different stabilisation times could be required so that the values are valid and can be used on the Darcy scale (Rücker et al., 2021).

Depending on the magnitude of the fluctuation amplitude, a different stabilisation time could be required. Repeating the different fractional flow steps multiple times shows that the distribution of water and oil

clusters are never the same, the global saturations are in agreement, but the local fluid distribution always has deviations, as shown in the following two studies (Pentland et al., 2011) and (Andrew et al., 2014b).

Relative permeability

The interpretation of the steady-state experiment for relative permeability is illustrated in Figure 7. The results show two sets of relative permeability curves of the oil-water system. The first one has fewer measured saturation points and corresponding relative permeability values. The second was the repetition of the first measurement with more measured points in the lower water saturation area.

The second set of measured values was necessary to understand better the fluid flow behaviour of the two-phase system at high oil saturation.

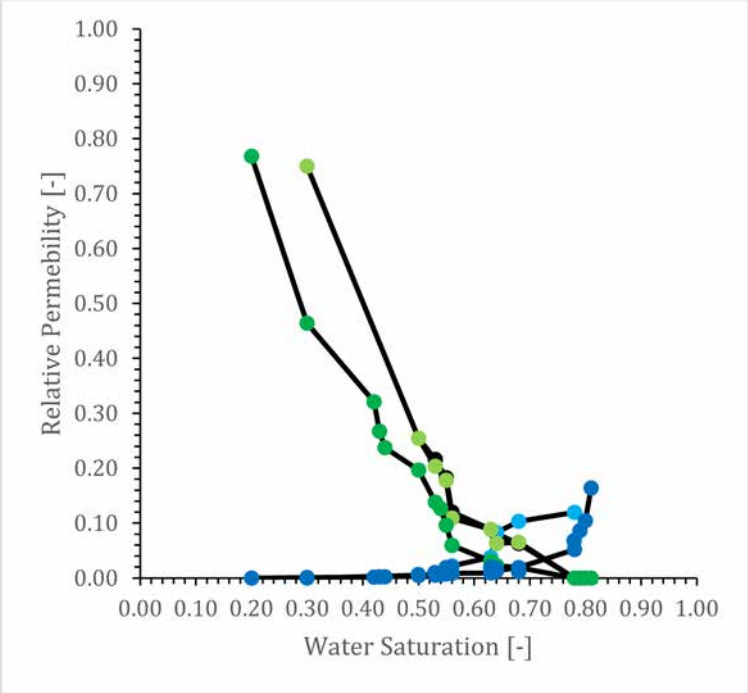

Figure 9—Relative permeability results for oil (green) and water (blue)

The results show that the analytically determined values agree with the proposed theory (Tang et al., 2019). The microfluidic approach showed additional advantages, such as the wettability and simultaneous determination of the imbibition capillary pressure as a function of water saturation.

With the application of the image analysis, the water saturations at the different fractional flow steps can be determined not only on the global scale but locally. The first results of the local fluid distributions along the core after different depletion stages are illustrated in Figure 10.

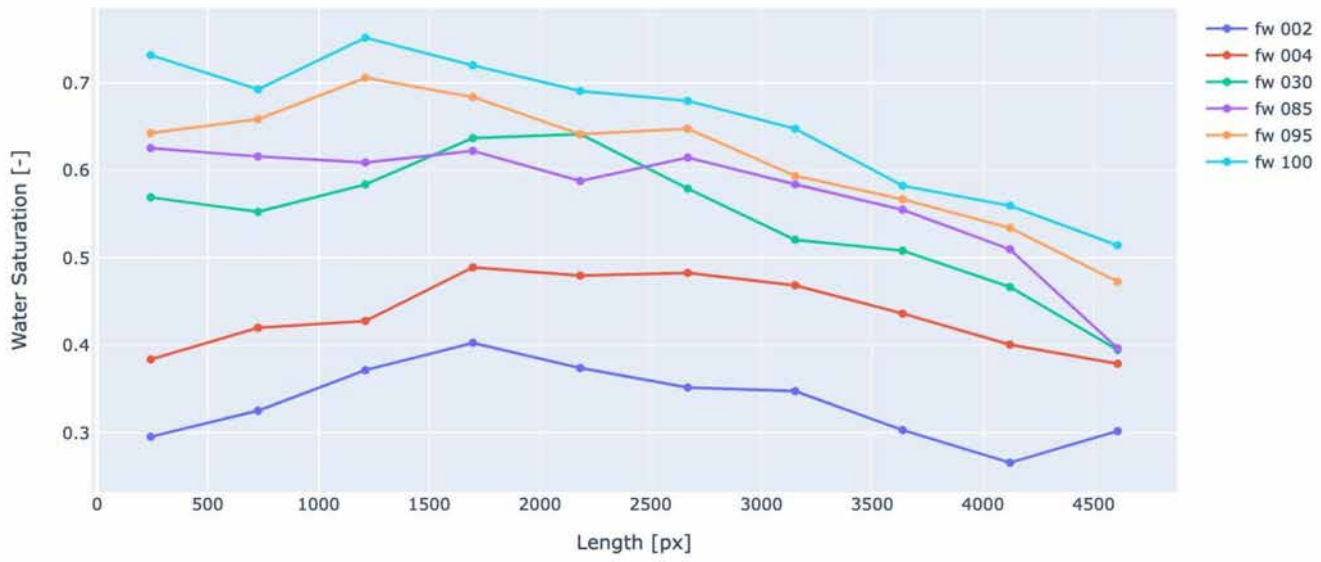

Figure 10—Example of water saturation distribution across the chip length

It means that sufficiently frequent imaging and continuously determined local fluid saturation changes could support understanding the pressure fluctuations. It requires further improvement of the image processing tool, most importantly automation, which is needed for processing relatively large amounts of data objectively and in a reasonable amount of time.

Contact angle and capillary pressure

The wettability and capillary pressure could be successfully determined from the captured images during the different flooding stages. In order to determine these two parameters, the contact angle needed to be analysed with image processing using only the data obtained from the steady-state method in a microchip. The contact angle could be determined at each saturation stage; the reason behind the contact angle change is not directly the altered water saturation. The direct reason for the contact angle change is the individual fluid velocity change, type of displacement (type of displacement, advancing vs receding angle), and radii of curvature due to the local porous media structure on the micro-level. The individual fluid velocities change during the different stages of the fractional flow. During the complete SCAL workflow, the total flow rate is constant, so the individual flow rates are changing, therefore the velocities, too. It starts with the maximum oil velocity and decreases, while the water velocity gradually increases. The contact angle increases with a higher water phase velocity (Samara & Jaeger, 2022). The higher contact angle means a change in wettability and capillary pressure. The contact angle is measured, and the capillary pressure values are calculated at each fractional flow step. The capillary pressure calculation results are illustrated in Figure 11.

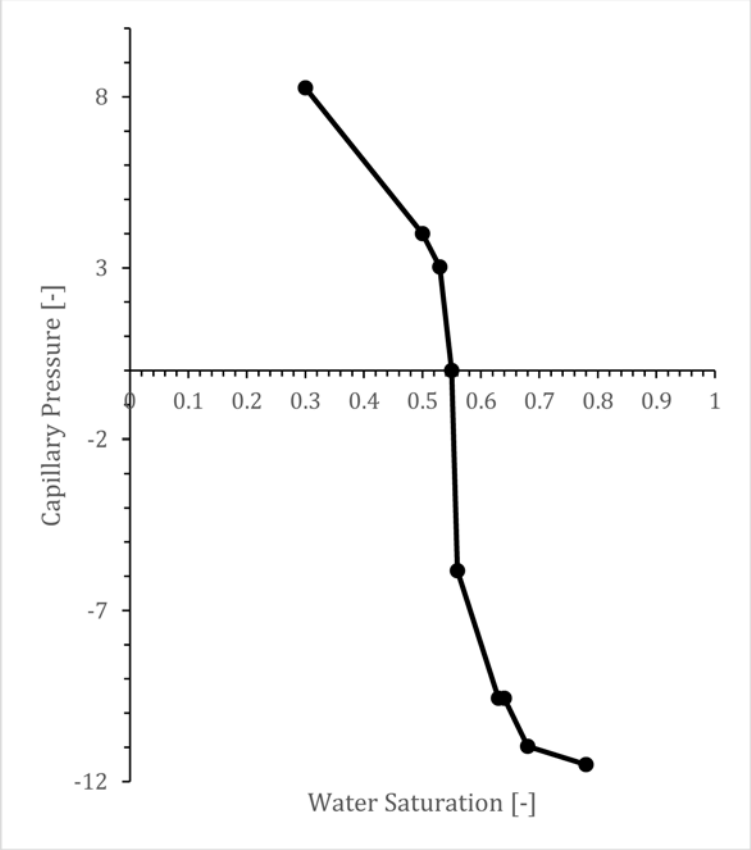

Figure 11—Capillary pressure results (during imbibition)

Currently, for the interpretation of capillary pressure the contact angle at different saturations is measured from the captured images. In order to arrive at a more representative contact angle value, all the possible locations should be captured for contact angle measurement, where the automation of the contact angle analysis could provide a more precise solution.

Conclusion

The simultaneous measurement of the relative permeability at different saturation stages and contact angles and as well as the capillary pressure determination are possible at the predefined stages, mimicking the natural depletion process of a hydrocarbon reservoir in a microchip, resembling synthetic porous media. Different saturation stages were reached with varying fractional flows, with a constant total flow rate, in a two-phase system consisting of light crude oil and distilled water. The results show the proof of concept that a simultaneous two-phase injection through two inlets into the micromodels is feasible. There are numerous economic and technical advantages of this approach.

Image processing contributes to developing an interpretation tool for estimating wettability and capillary pressure. The application of microfluidic setup and image analysis could provide further possibilities to derive mathematical models for the relationship between the different multi-phase flow characteristics. Investigation of different porous media patterns could be useful. It provides the possibility of generalising the established functions between the measured properties with sufficient experiments, using micromodel design based on realistic pore structures that closely resemble real rock samples. The SCAL on-chip could be a feasible solution to overcome both technical and economic limitations of digital rock physics or at least to serve as an additional source of information.

Future steps may include comparing the result of SCAL measurement in the core and micromodel flooding experiments, starting with Bentheimer sandstone from (Gaol et al., 2020) and where numerous

literatures are available for instance (Shikhov et al., 2017) and (Lin et al., 2019). Another potential interest is in applying machine learning, specifically Convolutional Neural Networks, for directly interpreting relative permeabilities from the snapshots of micromodel flooding images.

Moreover, the understanding of the two-phase fluid displacement needs to be further examined on pore-scale. The encountered micro-scale phenomena point to the future direction of this research, where understanding and investigating the possible causes that drive the fluctuations and clustering is the main goal. The observed phenomena could be further analysed during microfluidic flooding in microchips to describe it on a macro scale to model the whole process.

Acknowledgement

The authors would like to thank IPS International LLS for providing the reservoir oil sample used for the experiments.

References

Andrew, M., Bijeljic, B., & Blunt, M. J. (2014a). Pore-scale contact angle measurements at reservoir conditions using X-ray microtomography. *Advances in Water Resources*, **68**(June), 24–31. https://doi.org/10.1016/j.advwatres.2014.02.014

Andrew, M., Bijeljic, B., & Blunt, M. J. (2014b). Pore-scale imaging of trapped supercritical carbon dioxide in sandstones and carbonates. *International Journal of Greenhouse Gas Control*, **22**, 1–14. https://doi.org/10.1016/J.IJGGC.2013.12.018

Blunt, M. J. (2017). Multiphase Flow in Permeable Media. In *Multiphase Flow in Permeable Media*. Cambridge University Press. https://doi.org/10.1017/9781316145098

Blunt, M. J., Bijeljic, B., Dong, H., Gharbi, O., Iglauer, S., Mostaghimi, P., Paluszny, A., & Pentland, C. (2013). Pore-scale imaging and modelling. *Advances in Water Resources*, **51**, 197–216. https://doi.org/10.1016/j.advwatres.2012.03.003

Bradski, G. (2000). The OpenCV Library. *Dr Dobb's Journal of Software Tools*.

Clark, A. (2015). Pillow (PIL Fork) Documentation. readthedocs. https://buildmedia.readthedocs.org/media/pdf/pillow/latest/pillow.pdf

der Walt, S., Schönberger, J. L., Nunez-Iglesias, J., Boulogne, F., Warner, J. D., Yager, N., Gouillart, E., & Yu, T. (2014). Scikit-Image: image processing in Python. *PeerJ*, **2**, e453.

Gao, Y., Lin, Q., Bijeljic, B., & Blunt, M. J. (2017). X-ray Microtomography of Intermittency in Multiphase Flow at Steady State Using a Differential Imaging Method. *Water Resources Research*, **53**(12), 10274–10292. https://doi.org/10.1002/2017WR021736

Gaol, C. L., Wegner, J., & Ganzer, L. (2020). Real structure micromodels based on reservoir rocks for enhanced oil recovery (EOR) applications. *Lab on a Chip*, **20**(12), 2197–2208. https://doi.org/10.1039/d0lc00257g

Ghazanfari, M. H., Khodabakhsh, M., Kharrat, R., Rashtchian, D., & Vossoughi, S. (2006). Unsteady State Relative Permeability and Capillary Pressure Estimation of Porous Media.

Khajepour, H., Mahmoodi, M., Biria, D., & Ayatollahi, S. (2014). Investigation of wettability alteration through relative permeability measurement during MEOR process: A micromodel study. *Journal of Petroleum Science and Engineering*, **120**, 10–17. https://doi.org/10.1016/j.petrol.2014.05.022

Lin, Q., Bijeljic, B., Berg, S., Pini, R., Blunt, M. J., & Krevor, S. (2019). Minimal surfaces in porous media: Pore-scale imaging of multi-phase flow in an altered-wettability Bentheimer sandstone. https://doi.org/10.1103/PhysRevE.99.063105

Masalmeh, S. K., Jing, X., Roth, S., Wang, C., Dong, H., & Blunt, M. (2015). Towards predicting multi-phase flow in porous media using digital rock physics: Workflow to test the predictive capability of pore-scale modeling. Society of Petroleum Engineers - Abu Dhabi International Petroleum Exhibition and Conference, ADIPEC 2015. https://doi.org/10.2118/177572-ms

Mcphee, C. (2015). Special Core Analysis: Challenges, Pitfalls and Solutions.

McPhee, C., Reed, J., & Zubizarreta, I. (2015). Best Practice in Coring and Core Analysis. *Developments in Petroleum Science*, **64**, 1–15. https://doi.org/10.1016/B978-0-444-63533-4.00001-9

Mejia, L., Tagavifar, M., Xu, K., Mejia, M., Du, Y., & Balhoff, M. (2019). Surfactant flooding in oil-wet micromodels with high permeability fractures. *Fuel*, **241**, 1117–1128. https://doi.org/10.1016/j.fuel.2018.12.076

Oldenburg, T. B. P., Jaeger, P., Gros, J., Socolofsky, S. A., Pesch, S., Radović, J. R., & Jaggi, A. (2019). Physical and Chemical Properties of Oil and Gas Under Reservoir and Deep-Sea Conditions. *Undefined*, 25–42. https://doi.org/10.1007/978-3-030-11605-7_3

Pentland, C. H., El-Maghraby, R., Iglauer, S., & Blunt, M. J. (2011). Measurements of the capillary trapping of supercritical carbon dioxide in Berea sandstone. https://doi.org/10.1029/2011GL046683

Rücker, M., Georgiadis, A., Armstrong, R. T., Ott, H., Brussee, N., van der Linde, H., Simon, L., Enzmann, F., Kersten, M., & Berg, S. (2021). The Origin of Non-thermal Fluctuations in Multiphase Flow in Porous Media. *Frontiers in Water*, **3**, 45. https://doi.org/10.3389/FRWA.2021.671399/BIBTEX

Samara, H., Al-Eryani, M., & Jaeger, P. (2022). The role of supercritical carbon dioxide in modifying the phase and interfacial properties of multi-phase systems relevant to combined EOR-CCS. *Fuel*, **323**(April), 124271. https://doi.org/10.1016/j.fuel.2022.124271

Samara, H., & Jaeger, P. (2022). Experimental determination of wetting behavior under non-atmospheric conditions relevant to reservoirs: a practical guide. *SN Applied Sciences*, **4**(3). https://doi.org/10.1007/s42452-022-04963-8

Shikhov, I., d'Eurydice, M.N., Arns, J.Y., & Arns, C.H. (2017). An Experimental and Numerical Study of Relative Permeability Estimates Using Spatially Resolved T1-z NMR. *Transport in Porous Media*, **2**(118), 225–250. https://doi.org/10.1007/S11242-017-0855-7

Tahir, M., Hincapie, R. E., Langanke, N., Ganzer, L., & Jaeger, P. (2020). Coupling microfluidics data with core flooding experiments to understand sulfonated/polymer water injection. *Polymers*, **12**(6). https://doi.org/10.3390/POLYM12061227

Tang, J., Smit, M., Vincent-Bonnieu, S., & Rossen, W. R. (2019). New Capillary Number Definition for Micromodels: The Impact of Pore Microstructure. *Water Resources Research*. https://doi.org/10.1029/2018WR023429

Wegner, J. (2015). Investigation of polymer enhanced oil recovery (EOR) in microfluidic devices that resemble porous media - An experimental and numerical approach. **41**(3), 137–142. https://www.amazon.com/Investigation-Enhanced-Recovery-Microfluidic-Resemble/dp/3844035206

Yang, D., Tontiwachwuthikul, P., & Gu, Y. (2005). Interfacial tensions of the crude oil + reservoir brine + CO2 systems at pressures up to 31 MPa and temperatures of 27°C and 58°C. *Journal of Chemical and Engineering Data*, **50**(4), 1242–1249. https://doi.org/10.1021/je0500227